J Solid State Electrochem (2005) 9: 438–444
DOI 10.1007/s10008-004-0593-y

ORIGINAL PAPER

Xiang Ming He · Jian Jun Li · Yan Cai · Yaowu Wang
Jierong Ying · Changyin Jiang · Chunrong Wan

# Preparation of spherical spinel $LiMn_2O_4$ cathode material for lithium ion batteries

Received: 19 July 2004 / Revised: 21 July 2004 / Accepted: 28 September 2004 / Published online: 15 December 2004


**Abstract** A novel process is proposed for synthesis of spinel $LiMn_2O_4$ with spherical particles from the inexpensive materials $MnSO_4$, $NH_4HCO_3$, and $NH_3{\bullet}H_2O$. The successful preparation started with carefully controlled crystallization of $MnCO_3$, leading to particles of spherical shape and high tap density. Thermal decomposition of $MnCO_3$ was investigated by both DTA and TG analysis and XRD analysis of products. A precursor of product, spherical $Mn_2O_3$, was then obtained by heating $MnCO_3$. A mixture of $Mn_2O_3$ and $Li_2CO_3$ was then sintered to produce $LiMn_2O_4$ with retention of spherical particle shape. It was found that if lithium was in stoichiometric excess of 5% in the calcination of spinel $LiMn_2O_4$, the product had the largest initial specific capacity. In this way spherical particles of spinel $LiMn_2O_4$ were of excellent fluidity and dispersivity, and had a tap density as high as 1.9 g $cm^{-3}$ and an initial discharge capacity reaching 125 mAh $g^{-1}$. When surface-doped with cobalt in a 0.01 Co/Mn mole ratio, although the initial discharge capacity decreased to 118 mAh $g^{-1}$, the 100th cycle capacity retention reached 92.4% at 25°C. Even at 55°C the initial discharge capacity reached 113 mAh $g^{-1}$ and the 50th cycle capacity retention was in excess of 83.8%.

**Keywords** Spherical particles · Spinel $LiMn_2O_4$ · Li-ion battery · Controlled crystallization · $MnCO_3$

## Introduction

Recent decades have witnessed the rapid development of the lithium-ion battery in response to the growing needs of the electronic and information industries. Exploration of new cathode material that is cost effective and environmentally benign, compared to $LiCoO_2$, has been extensively attempted. Its non-toxic property and low cost make spinel $LiMn_2O_4$ an attractive alternative to $LiCoO_2$. Solid-phase reaction to prepare spinel $LiMn_2O_4$ was first adopted by Hunter [1], and was improved by Tarascon, Thackeray, Kosova, and Soiron [2–6]. Solid-phase reaction combined with milling is currently widely used to prepare spinel $LiMn_2O_4$ materials. Other conventional methods of preparation are sol–gel [7] and co-precipitation [8, 9]. The spinel $LiMn_2O_4$ powders obtained by use of these methods always have irregular particles with broad size distribution. Unfortunately, little attention has been paid to particle morphology, which has an important effect on the characteristics of spinel $LiMn_2O_4$. It has been found that regular quasi spherality of particles could significantly enhance the performance of spinel $LiMn_2O_4$ [10, 11]. Sintering took long time, however, and the particles obtained had a wide size range and irregular surface, which was not beneficial to surface modification. Spherical particles of spinel $LiMn_2O_4$ could lead to high tap density, which affects the energy density of the battery, and uniform surface coating, which is an effective way of enhancing performance.

Our laboratory has been engaged in developing high-density electrode materials with spherical particles by a process named controlled crystallization since 1995, and has prepared $Ni(OH)_2$ for Ni-MH batteries [12, 13], $LiCoO_2$ [14] and $LiNi_{0.8}Co_{0.2}O_2$ [15], all with spherality. It is found that the spherical powders have excellent fluidity and dispersivity and much higher tap density, which is advantageous for preparation of electrodes. Surface coating of spherical powders is also much more effective than for non-spherical. The surface coating on spherical particles is well distributed, stable, and firm [16]. Therefore, preparing spherical powder should be a useful way to high-performance spinel $LiMn_2O_4$.

X. M. He (✉) · J. J. Li · Y. Cai · Y. Wang · J. Ying
C. Jiang · C. Wan
Materials Chemistry Lab, INET, Tsinghua University,
P.O. Box 1021, Beijing, 102201, PR China
E-mail: hexm@tsinghua.edu.cn
Tel.: +86-10-89796073
Fax: +86-10-69771464

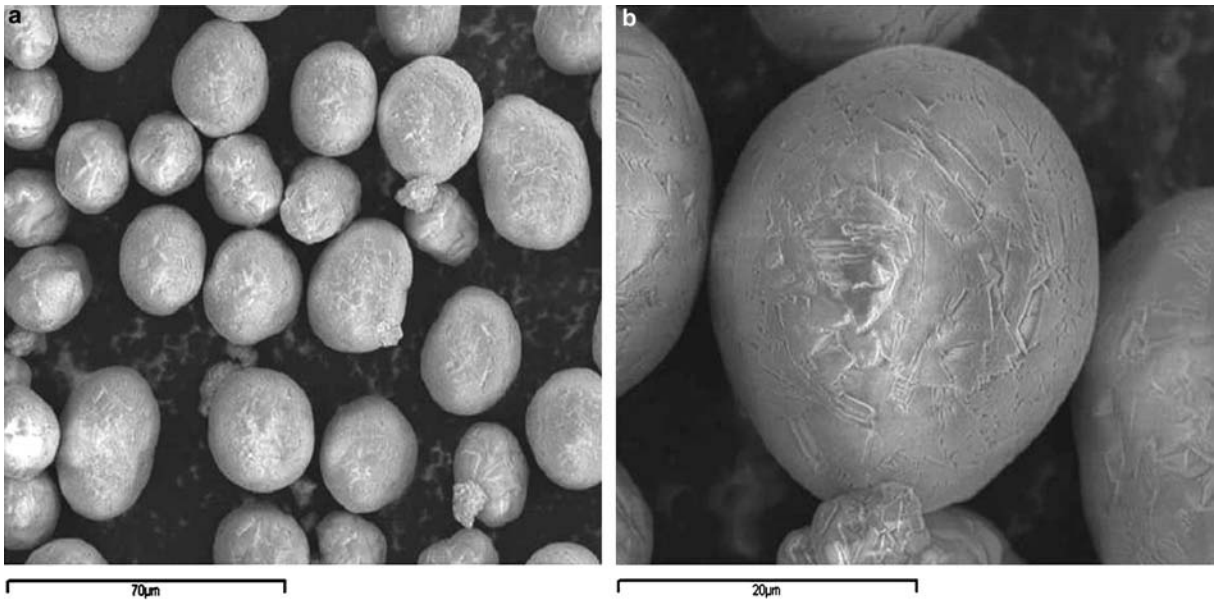


**Fig. 1** Scanning electron microscopic images of $MnCO_3$ powders

In this study, thermal decomposition of $MnCO_3$ was investigated by DTA, TG, and XRD. Starting with spherical $MnCO_3$ powders obtained by controlled crystallization, spherical spinel $LiMn_2O_4$ powders were prepared by sintering to obtain spherical $Mn_2O_3$ powders then sintering a mixture of as-obtained $Mn_2O_3$ and $Li_2CO_3$. Cobalt surface doping on spherical spinel $LiMn_2O_4$ powders was carried out and the electrochemical performance of the products was tested.

## Experimental

First, spherical $MnCO_3$ powders was prepared. The $MnCO_3$ was precipitated with ammonium carbonate:

$$MnSO_4 + 2NH_4HCO_3 = MnCO_3 \downarrow + (NH_4)_2SO_4 + H_2CO_3$$

Solutions of $MnSO_4 \bullet H_2O$, $NH_4HCO_3$, and aqueous ammonia were fed continuously by peristaltic pumps into a crystallization reactor with agitation. The resulting suspension with $MnCO_3$ precipitate overflowed out of the reactor. Here, $NH_3$ was used as the complexing agent. The concentration of the solutions, flow rates, agitating intensity, temperature, and pH of the solution in the reactor were optimized and controlled carefully. Under these conditions, all particles gradually adopt a spherical shape if reaction time is sufficient and under proper agitation. The solid in the overflow suspension solution was spherical $MnCO_3$ powder. It was isolated by centrifugation and washed, rinsed, and dried before further processing.

The spherical $Mn_2O_3$ intermediate was then obtained by heat-treatment of $MnCO_3$ at 560 °C for 4 h. This was then mixed with $Li_2CO_3$ and the mixture was calcined to produce $LiMn_2O_4$ by heat-treatment as follows:

1 heating from room temperature to 560°C in 2 h and holding for 4 h,
2 heating from 560 to 750 °C in 1 h and holding for 20 h, and
3 cooling by exposure to air at room temperature.

Cobalt surface doping was conducted as follows. The $Mn_2O_3$ obtained was added to deionized water and agitated to form a suspension. $CoSO_4$ solution was fed into the agitated suspension and LiOH solution was also fed slowly into the agitating suspension, in accordance with $[Co^{2+}]/[OH^-] = 1/2$. Thus, $Co(OH)_2$ was coated on the spherical $Mn_2O_3$ particles. The coated $Mn_2O_3$ was then sintered with $Li_2CO_3$ to prepare cobalt-doped spinel $LiMn_2O_4$ by the same heating program as described above.

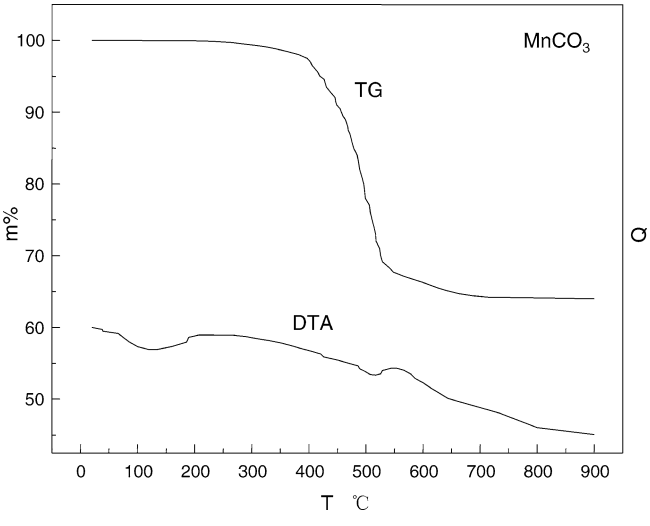


**Fig. 2** TG/DTA curves of spherical $MnCO_3$

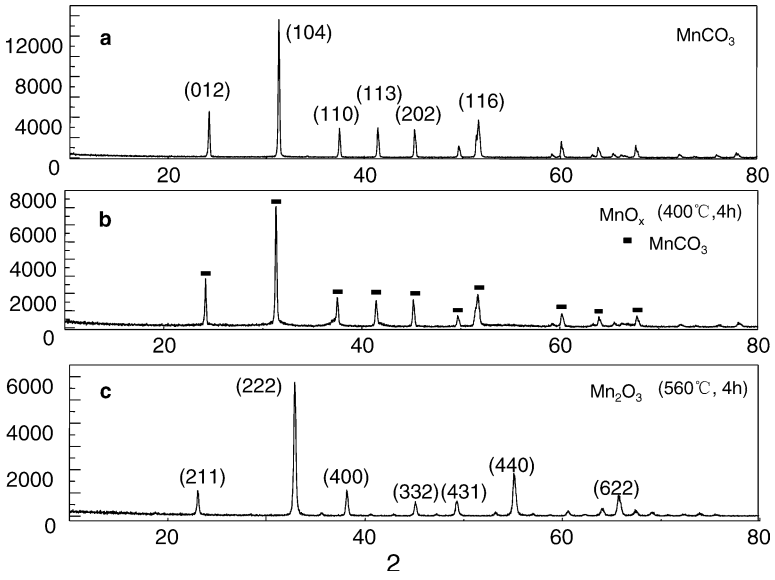


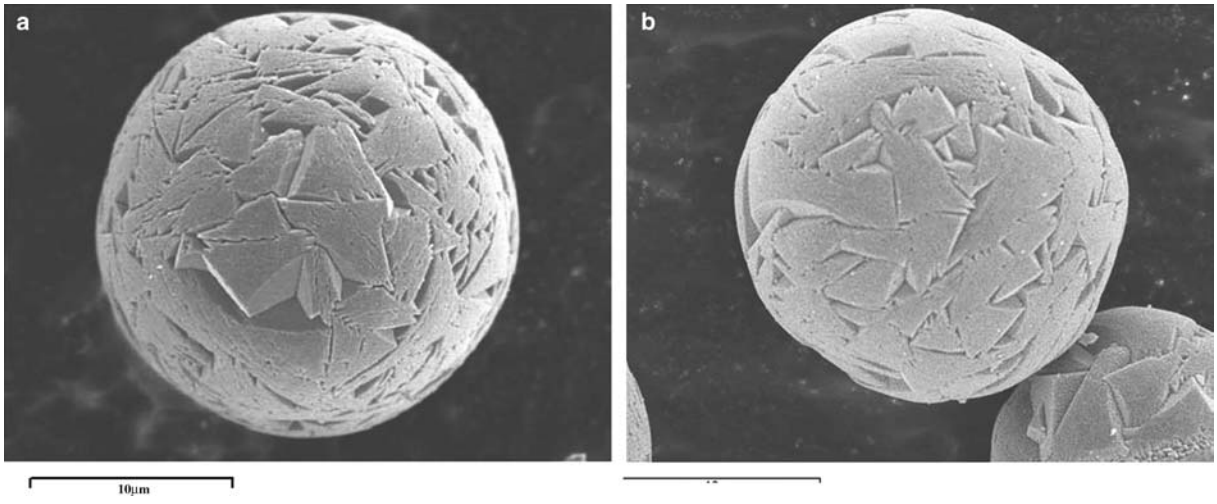


**Fig. 3** X-Ray diffraction patterns: **a** spherical $MnCO_3$, **b** heated at 400 °C, **c** heated at 560 °C for 4 h

**Fig. 4** Scanning electron microscopy images of spherical $MnCO_3$ heated at 400 °C (**a**) and at 560 °C (**b**) with a scale indicating 10 μm

DTA and TG analysis was performed with a PCT-1 thermal analyzer. The rate of heating was kept at 10°C $min^{-1}$. The phase composition of the powders was characterized by powder X-ray diffraction (XRD; D/max-rB) using CuK$\alpha$, 40 kV, 120 mA, with steps of 0.02° at 6° $min^{-1}$. The particle morphology of the powders was observed by use of scanning electron microscopy (SEM; JSM6301F). The tap-density of the powders was tested by using a method described elsewhere [17].

The electrode formulation consisted of 80% (*w*/*w*) $LiMn_2O_4$, 10% (*w*/*w*) carbon black, and 10% (*w*/*w*) binder. The loading of $LiMn_2O_4$ was about 10 mg $cm^{-2}$. The prepared electrode pellets were dried at 120°C under vacuum for 48 h. The test coin cells were assembled in a dry glove box filled with argon. The separator was a Celguard 2400 microporous polypropylene membrane. The electrolyte was 1 mol $L^{-1}$ $LiPF_6$ in EC + DEC (1:1, *v*/*v*). A lithium metal anode was used in this study. The charge–discharge cycling was galvanostatically performed at a current of 0.5 mA $cm^{-2}$ with cut-off voltages of 3.35–4.35 V at room temperature and with cut-off voltage of 3.35–4.2 V at 55°C.

## Results and discussion

### Thermal decomposition of $MnCO_3$

Figure 1 shows the SEM images of spherical $MnCO_3$. Its tap density and particle size were 2.1 g $cm^{-3}$ and approximate 20 μm, respectively. The spherical $MnCO_3$ sample is of excellent fluidity and dispersivity, and the surfaces look close-grained and compact.

An attempt was made to prepare spinel $LiMn_2O_4$ by sintering a mixture of $MnCO_3$ and $Li_2CO_3$, but the sample obtained had a low first discharge specific capacity of 106 mAh $g^{-1}$ and poor cycleability with loss of 6 mAh $g^{-1}$ after ten cycles.

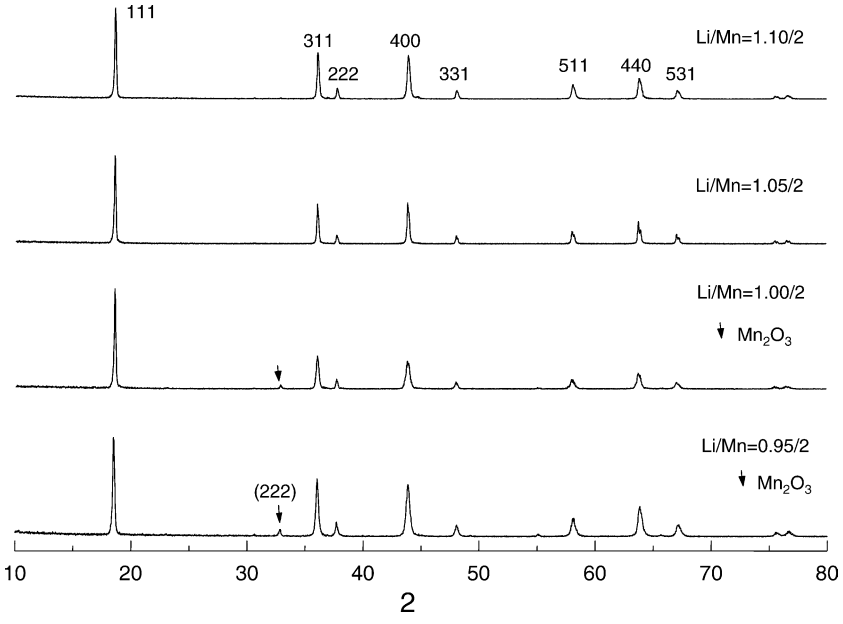


**Fig. 5** X-Ray diffraction patterns of spinel $LiMn_2O_4$ with different mole ratios of Li/Mn

It is said that $MnCO_3$ can be transformed to $MnO_2$ by heating at 400 °C [19]. It is found experimentally that this transformation needs a long sintering time, which is costly. Thus it was necessary to investigate pyrolysis of $MnCO_3$. Figure 2 presents DTA and TG results for spherical $MnCO_3$. The DTA curve contains a first endothermal peak at about 120°C, where water evaporates, a slow endothermal range from 300 to 520°C, where decomposition of $MnCO_3$ occurs and $CO_2$ is given off, and two sharp endothermal peaks at 420 and 520°C, which correspond to the decomposition of $MnCO_3$ to $MnO_2$ and the transformation of $MnO_2$ to $Mn_2O_3$, respectively. Corresponding mass changes are observed in the TG curve. The mass loss starts at about 300°C, accelerates from 400 to 520°C, and achieves a constant level of 32% at about 560°C, at which temperature decomposition of $MnCO_3$ to $Mn_2O_3$ is complete.

The probable mechanism of decomposition of spherical manganese carbonate is divided into two steps. First, decomposition to $MnO_2$ and $CO_2$ starts at about 300°C and accelerates from 400 to 520°C. Then $MnO_2$ is transformed to $Mn_2O_3$ at about 520°C. These processes can be described by the equations:

$$2MnCO_3 + O_2 = 2MnO_2 + 2CO_2 \uparrow \quad (1)$$

$$4MnO_2 = 2Mn_2O_3 + O_2 \uparrow \quad (2)$$

Because of the compact spherical particles of $MnCO_3$, with diameters in excess of 20 μm, the reaction in Eq. (1) starts on the surface of particle and moves gradually into center. Emission of $CO_2$ leaves interstices behind, as shown in Fig. 4, which accelerates inner decomposition. So decomposition of spherical $MnCO_3$ particles to $MnO_2$ happens gradually from 300 to 520°C. Meanwhile, the reaction in Eq. (2) starts at about 520°C. The theoretical mass loss for complete decomposition of $MnCO_3$ to $Mn_2O_3$ is 31.3%, which fits well the experimental data of 32%.

The XRD patterns recorded for spherical $MnCO_3$ powder and after heating at 400 and 560°C are illustrated in Fig. 3. It is apparent from the similarity of Figs. 3a and 3b that most of the crystals of $MnCO_3$ remain when heated at 400°C. The decrease in the height of the lines in Fig. 3b compared with Fig. 3a shows that decomposition of $MnCO_3$ occurs at 400°C. New, weak unorderly lines near the baseline of Fig. 3b also show that a new crystal phase with low crystallinity forms when $MnCO_3$ is heated at 400°C. Figure 3c shows that decomposition is complete at 560°C and all the material remaining is cubic $Mn_2O_3$.

The SEM image of $Mn_2O_3$ powder is shown in Fig. 4b. The morphology of spherical $Mn_2O_3$ looks no different from that of $MnCO_3$ heated at 400 °C (Fig. 4a). This lack of difference shows that decomposition of $MnCO_3$ progresses in the inner part of particles after 400 °C. When heated at 560 °C, the surface of particle chips and is much coarser than that of $MnCO_3$.

This analysis shows that pyrolysis of $MnCO_3$ should be performed at 560 °C for 4 h.

## Calcination of spinel $LiMn_2O_4$

TG/DTA analysis of the mixture of $Mn_2O_3$ and $LiCO_3$ shows that an endothermic peak occurs at 560°C; this corresponds to the reaction between $Mn_2O_3$ and $LiCO_3$. According to Zhang [18] the optimum temperature for the best electrochemical performance of spinel $LiMn_2O_4$ is 750 °C.

In this work the best temperature program for calcination of spinel $LiMn_2O_4$ was found to be:

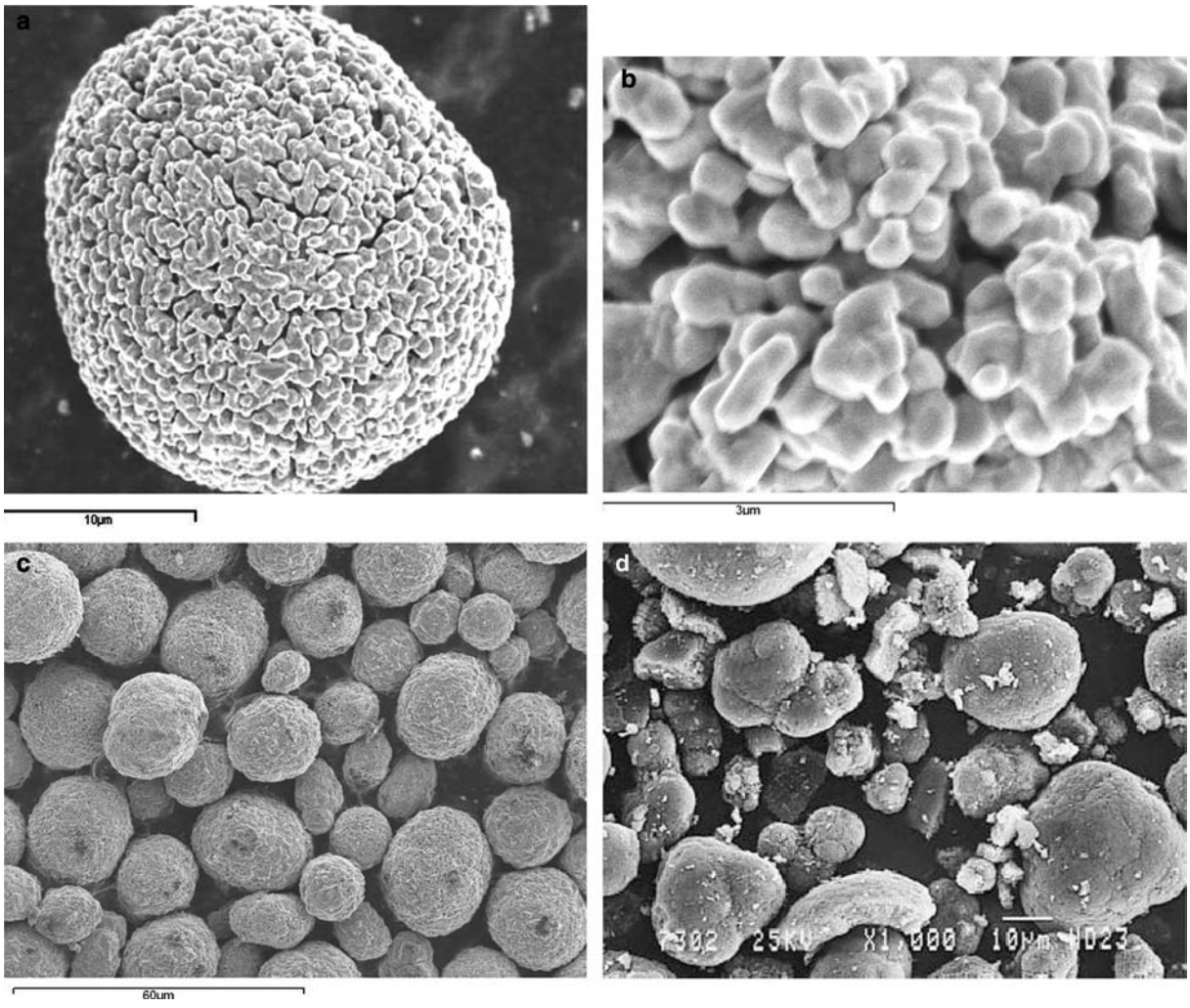


**Fig. 6** Scanning electron microscopy images of the obtained spinel $LiMn_2O_4$: **a** one particle, with a scale indicating 10 μm, **b** the surface, with a scale indicating 3 μm, **c** the powder, with a scale indicating 60 μm, **c** the Merck product, from Ref. [11], with a scale indicating 10 μm

1 heating from room temperature to 560°C in 2 h and holding for 4 h;
2 heating from 560 to 750°C in 1 h and holding for 20 h; and
3 cooling by exposure to air at room temperature.

This sintering time is shorter than that of the Merck product [11] .

Samples of spinel $LiMn_2O_4$ were prepared by use of this program and Li/Mn mole ratios of 0.95/2, 1.00/2, 1.05/2, and 1.10/2. As shown in Fig. 5, the XRD patterns for the samples with ratios 0.95/2 and 1.00/2 have a diffraction line (222) corresponding to $Mn_2O_3$, and this is weaker for the sample with ratio 1.00/2. This indicates there is a lithium deficiency in the mixture with a stoichiometric amount of $L_2CO_3$, probably because of loss of lithium during calcination. A slight excess of lithium should thus be used to furnish a single-phase product. The diffraction line (222) corresponding to $Mn_2O_3$ disappears from the patterns for samples with Li/Mn mole ratios 1.05/2 and 1.10/2; this shows that they are pure phase of spinel $LiMn_2O_4$. Lithium should therefore be in stoichiometric excess of 5% for calcination of spinel $LiMn_2O_4$.

Electrochemical performance showed that the largest initial discharge specific capacity, in excess of 125 mAh $g^{-1}$, was obtained for the sample with an Li/Mn mole ratio of 1.05/2. This ratio was thus adopted for preparation of spherical spinel $LiMn_2O_4$ powder by calcination of $Mn_2O_3$ and $Li_2CO_3$.

Figure 6 shows SEM images of the spinel $LiMn_2O_4$ obtained and the Merck product [11]. Its surface morphology (Fig. 6a) is the same as that reported in Ref. [18], and it keeps the shape and size of the precursor $MnCO_3$. Obviously, the particle is compactly made up of a large number of granular crystalline grains of spinel $LiMn_2O_4$, the sizes of which are 100 nm. The lax pile density and tap density of the obtained spinel $LiMn_2O_4$ were measured and found to be in excess of 1.6 and 1.9 g $cm^{-3}$. Those of the commercial product from market were found to be 1.1 and 1.9 g $cm^{-3}$. Because its particles are irregular and non-spherical, its lax pile density is generally much smaller than its tap density;

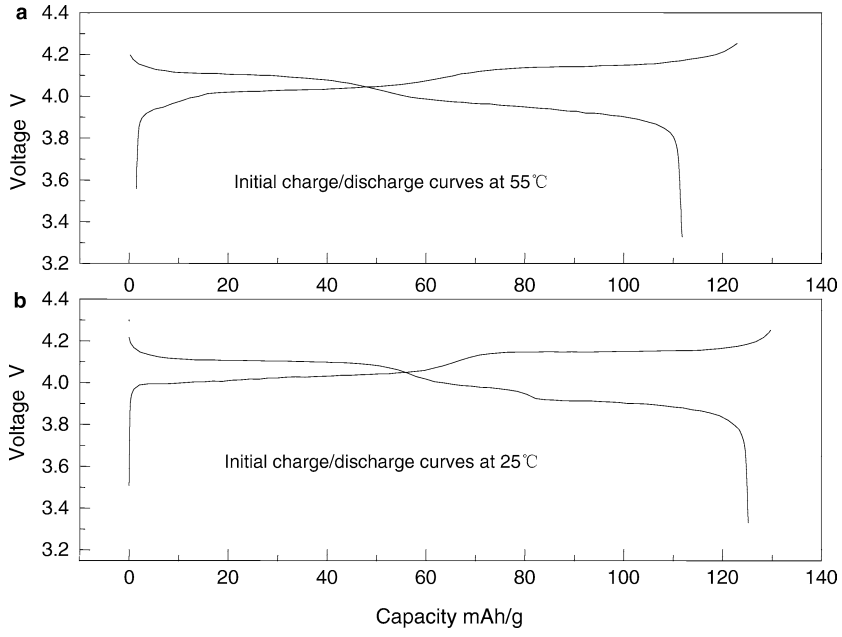


**Fig. 7** Initial charge/discharge curves of spherical spinel $LiMn_2O_4$ at 0.4 A

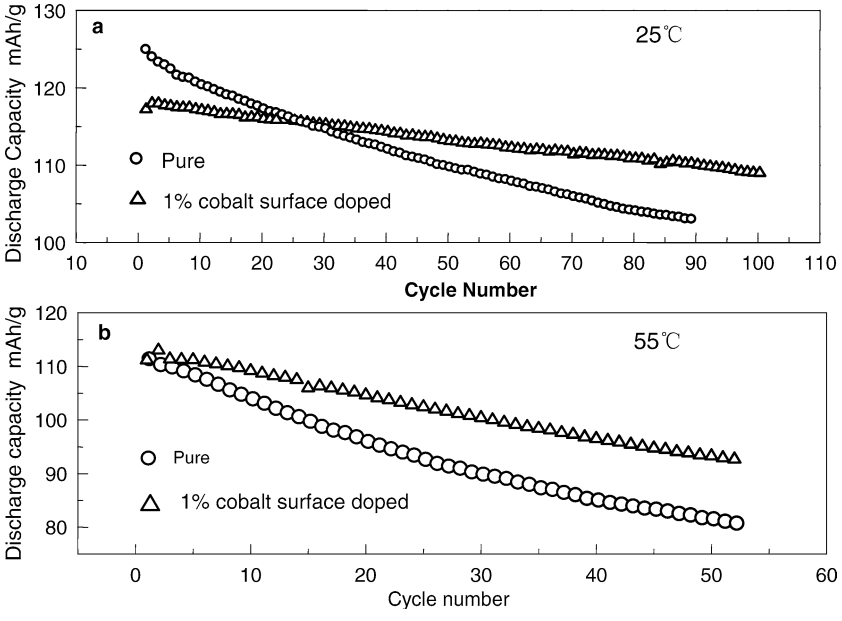


**Fig. 8** Cycleability of pure and doped $LiMn_2O_4$ at 0.4 A

this is not so for the spherical particles. Also, all the particles are spherical (10–25 μm) (Fig. 6c) whereas the Merck product (Fig. 6d) is a mixture of grains of different shape (10–60 μm).

## Performance of spinel $LiMn_2O_4$

As illustrated in Fig. 7, the spherical spinel $LiMn_2O_4$ powders obtained had a initial charge specific capacity of 131 and 125 mAh $g^{-1}$, followed by discharge capacities of 125 and 112 mAh $g^{-1}$ at 25 and at 55°C, respectively, at a current of 0.4 A.

The cycling performance of the spherical spinel $LiMn_2O_4$ is shown in Fig. 8. Its capacity remains to be 104 mAh $g^{-1}$ at the 100th cycle at 25 °C, and 82 mAh $g^{-1}$ at the 50th cycle at 55°C. Capacity retention is 83.3% at 100th cycle at 25°C and 73.3% at the 50th cycle at 55°C. When doped with 1% cobalt on the surface, retention increases to 92.4 and 83.8%, respectively, as shown in Fig. 8. Spherical spinel $LiMn_2O_4$ surface-doped with 1% cobalt has the same retention of capacity at the 40th cycle at 25°C as that of $LiCoO_2$ reported in Ref. [14]

The surface contact of a spherical particle with an electrolyte is generally less than for non-spherical particle. Less surface contact reduces dissolution of manganese in the electrolyte and improves performance during cycling. Doping with 1% cobalt, especially on the surface of spherical spinel $LiMn_2O_4$, can effectively

prevent manganese from dissolving in the electrolyte and improve cycleability at both 25 and at 55°C.

The spherical spinel $LiMn_2O_4$ cathode material with surface modification is thus a very promising candidate for use in lithium ion batteries at greatly reduced cost and with low risk of toxicity.

## Conclusions

The spinel $LiMn_2O_4$ with spherical particles has been successfully synthesized by the proposed process based on controlled crystallization. Spherical $MnCO_3$ powder with good fluidity and high density can be prepared by carefully controlled crystallization. Analysis of TG/DTA and XRD patterns shows that pure phase spherical $Mn_2O_3$ powders can be obtained by heating spherical $MnCO_3$ particles at 560°C for 4 h in air. A mixture of spherical $Mn_2O_3$ particles and $Li_2CO_3$ powder with an optimized Li/Mn ratio of 1.05/2 is then calcined to produce spherical particles of spinel $LiMn_2O_4$ by the proposed procedure. The product tap density is as high as 1.9 g $cm^{-3}$, its initial discharge capacity is in excess of 125 mAh $g^{-1}$ at 25°C, and its cycleability, at both 25 and 55°C, can be greatly improved by cobalt surface doping.

This process is cost-effective, because it uses the inexpensive materials $MnSO_4$, $NH_4HCO_3$, $NH_3{\bullet}H_2O$, and $Li_2CO_3$. It is also practical for industry-scale production. The spherical particles obtained are suitable for further surface modification. This paves the way to simple and economic production of spinel $LiMn_2O_4$ materials for advanced lithium ion batteries.

## References


1. Hunter James C (1981) J Solid State Chem 39:142
2. Tarascon JM, McKinnon WR, Coowar F, Bowmer TN, Amatucci G, Guyomard D (1994) J Electrochem Soc 141:1421
3. Thackeray MM, Shao-Horn Y, Kahaian AJ, Kepler KD, Skinner E, Vaughey JT, Hackney SA (1998) Electrochem Solid State Lett 1:7
4. Kosova NV, Devyatkina ET, Kozlova SG (2001) J Power Sources 97–98:406
5. Soiron S, Rougier A, Aymard L, Tarascon JM (2001) J Power Sources 97–98:402
6. Kosova NV, Uvarov NF, Devyatkina ET, Avvakumov EG (2000) Solid State Ionics 135:107
7. Bach S, Pereira-Ramos JP, Baffier N, Messina R (1992) Electrochim Acta 37:1301
8. Barboux P, Shokoohi FK, Tarascon JM (1992) US patent 5135732
9. Qiu XP, Sun XG, Shen WC, Chen NP (1997) Solid State Ionics 93:335
10. Levi E, Levi MD, Salitra G, Aurbach D, Oesten R, Heider U, Heider L (1999) Solid State Ionics 126:109
11. Aurbach D, Levi MD, Gamulski K, Markovsky B, Salitra G, Levi E, Heider U, Heider L, Oesten R (1999) J Power Sources 81–82:472
12. Jiang CY, Wan CR, Zhang Q, Zhang JJ (1997) Chin J Power Sources 21:243
13. Jiang CY, Zhang Q, Du XH, Wan CR (2000) Chin J Power Sources 24:207
14. Ying JR, Jiang CY, Wan CR (2004) J Power Sources 129:264
15. Ying JR, Jiang CY, Wan CR (2001) J Power Sources 99:78
16. Du XH, Jiang CY, Wan CR (2001) J Tsinghua Univ (Sci Technol) 41:71
17. Wan CR, Jiang CY (1998) J Tsinghua Univ (Sci Technol) 38:95
18. Zhang GY (2002) Doctoral dissertation, Tsinghua University
19. You BC (2001) China's Manganese Industry 19:11